ACS APPLIED MATERIALS & INTERFACES

Research Article

www.acsami.org

Quaternary Zn–Ag–In–Se Quantum Dots for Biomedical Optical Imaging of RGD-Modified Micelles

Dawei Deng,*[,†,‡] Lingzhi Qu,[†] Jian Zhang,*[,§] Yuxiang Ma,[†] and Yueqing Gu*[,†]

[†]Department of Biomedical Engineering, School of Life Science and Technology, China Pharmaceutical University, Nanjing 210009, China

[‡]Chemical Engineering Department, University of Michigan, Ann Arbor, Michigan 48109, United States

[§]Department of Pharmaceutical Sciences, College of Pharmacy, University of Michigan, Ann Arbor, Michigan 48109, United States

Supporting Information

ABSTRACT: Exploring the synthesis of new biocompatible quantum dots (QDs) helps in overcoming the intrinsic toxicity of the existing QDs composed of highly toxic heavy metals (e.g., Cd, Hg, Pb, etc.) and is particularly interesting for the future practical application of QDs in biomedical imaging. Hence, in this report, a new one-pot approach to oil-soluble (highly toxic heavy metal-free) highly luminescent quaternary Zn–Ag–In–Se (ZAISe) QDs was designed. Their photoluminescence (PL) emission could be systematically tuned from 660 to 800 nm by controlling the Ag/Zn feed ratio, and their highest PL quantum yield is close to 50% after detailed optimization. Next, by using biodegradable RGD peptide (arginine–glycine–aspartic acid)-modified *N*-succinyl-*N*′-octyl-chitosan (RGD-SOC) micelles as a water transfer agent, the versatility of these quaternary ZAISe QDs for multiscale bioimaging of micelles (namely, *in vitro* and *in vivo* evaluating the tumor targeting of drug carriers) was further explored, as a promising alternative for Cd- and Pb-based QDs.

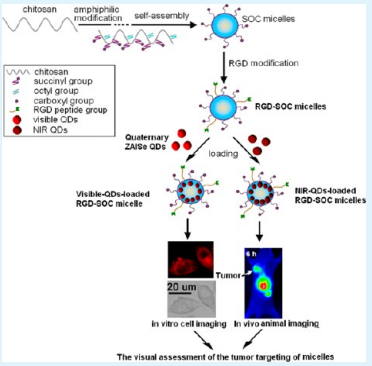

KEYWORDS: *quaternary quantum dots, Zn–Ag–In–Se, RGD-modified micelles, optical imaging, targeted delivery*

1. INTRODUCTION

Optical imaging has been a crucial biomedical imaging technique for the preclinical and clinical assessment of biological and biochemical processes.[1,2] Unlike other imaging techniques, this modality uses low-energy visible or near-infrared (NIR) light as the excitation and detection signals. As a result, optical methods can be used for biological imaging across multispatial scales, including cells, tissues, and small animals.[1−5] In particular, visible light can be widely applied for *in vitro* microscopy of cells, while NIR light (700–900 nm) is quite useful for *in vivo* imaging of small animals because of its deeper penetration into tissue.

To the best of our knowledge, optical imaging methods strongly rely on the development of fluorescent probes, because they usually use fluorescence as a molecular labeling (or imaging) signal.[3,4] As such, over the past decades, various fluorescent probes, such as organic dyes,[3,4] inorganic quantum dots (QDs),[4−7] etc., have been developed. Compared with traditional organic dyes, inorganic QDs exhibit many unique size-dependent optical and electronic properties.[3−7] However, most luminescent QDs used commonly for bioimaging are binary II–VI or IV–VI QDs containing highly toxic elements (e.g., Cd, Hg, Pb, etc.).[6−8] These toxic components have been proven to be eventually released into the cellular environment, inducing unsolvable cytotoxicity (the toxicity of elements used should be an important aspect for the issue of cytotoxicity of nanomaterials, besides the potential toxicity induced by their nanoscale structures). This is one of major obstacles to the future practical application of QDs and has inspired the search for novel alternative biocompatible ones.[8−10]

Ternary I–III–VI_2 QDs (where I = Cu or Ag, III = Ga or In, and VI = S or Se) and their alloys are among the most suitable alternatives to Cd-, Hg-, and Pb-based binary ones because of their similar favorable optoelectronic properties as well as their low toxicity.[9,10] In this family of semiconductors, considerable attention has been paid to $CuInS_2$ and $CuInSe_2$ (the Cu-based systems) and $AgInS_2$ (the Ag-based system) QDs.[9−18] Generally, most of the produced naked ternary QDs did not exhibit strong photoluminescence (PL) emission.[9−18] To further improve the PL property of these ternary QDs, a new efficient facile strategy is to fabricate novel quaternary Zn–I–III–VI nanostructures [e.g., PL quantum yields (QYs) of >70% for the quaternary Zn–Cu–In–S QDs],[19−23] which is receiving an increasing level of attention, as compared with the traditional ZnS (or CdS) overcoating strategy.[9−18]

As described above, most high-quality QDs are prepared in nonpolar organic media and thus have a hydrophobic surface. This might limit their applications in biomedical fields.[6,7] Here, we found that the micelles modified by bioactive ligands (e.g., folate, RGD peptide, etc.), the promising targeted delivery

Received: July 26, 2013
Accepted: October 1, 2013
Published: October 1, 2013

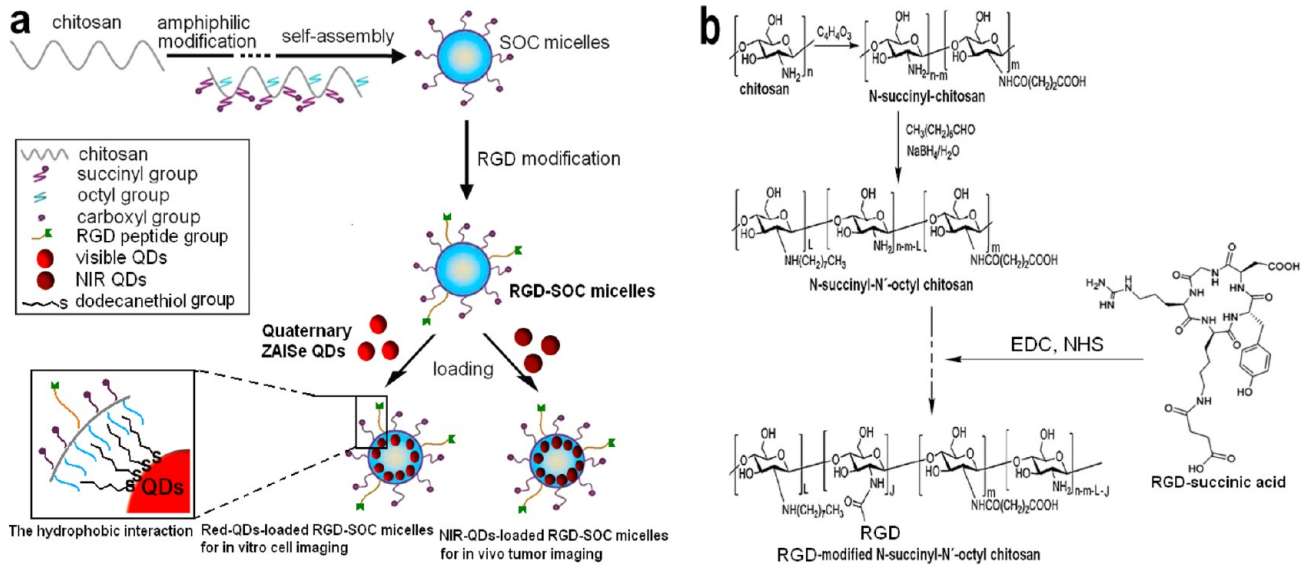

Figure 1. (a) Overall synthetic scheme for the QD-loaded RGD-SOC micelles. (b) Synthetic scheme for RGD-modified *N*-succinyl-*N*′-octyl-chitosan (SOC).

carriers for hydrophobic anticancer agents, have a hydrophobic core and a hydrophilic shell, in which their hydrophobic cores could be used to upload hydrophobic QDs because of the hydrophobic interaction.[13,24,25] Capitalizing on these cognitions, (i) we synthesized high-quality oil-soluble biocompatible quaternary alloyed Zn−Ag−In−Se QDs based on ternary $AgInSe_2$ with a bulk band gap of 1.24 eV[9] via a facile one-pot synthetic strategy, (ii) using monomeric cyclic RGD peptide-modified chitosan-based micelles, we transferred the oil-soluble quaternary Zn−Ag−In−Se (ZAISe) QDs into water successfully while retaining their fluorescence, morphology, and internal crystal structure, and (iii) finally, using *in vitro* cell and *in vivo* NIR imaging techniques, we demonstrated that these quaternary QDs are a versatile fluorescent probe for visual monitoring the tumor targeting of RGD-modified micelles in cells and mice. Here, it is worth mentioning that in the previous reports, to assess the same thematic issues, two organic dyes with different PL emissions were needed, e.g., fluorescein with green emission for *in vitro* cell imaging and cypate with NIR emission for *in vivo* small animal imaging.[25−27] Hence, these studies should be very interesting for developing new QD-based fluorescent probe for biomedical imaging.

2. EXPERIMENTAL SECTION

2.1. Materials. Zinc acetate [$Zn(Ac)_2$, 99.99%], silver nitrate ($AgNO_3$, >98%), indium acetate [$In(Ac)_3$, 99.99%], Se powder (100 mesh, 99.5%), 1-octadecene (ODE, 90%), oleic acid (OA, 90%), 1-dodecanethiol (DDT, 98%), oleylamine (OLA, 97%), chitosan (100 kDa), succinic anhydride (98%), octaldehyde (99%), monomeric cyclic RGD peptide, 1-ethyl-3-[3-(dimethylamino)propyl]-carbodiimide hydrochloride (EDC), and *N*-hydroxysuccinimide (NHS) were commercially available products and used as received [deionized water (18.2 MΩ cm) was used]. The NIR dye cypate was provided by S. Achilefu (Figure S6 of the Supporting Information).[28,29]

Human breast cancer cell lines MDA-MB-231 and MCF-7 (American Type Culture Collection, Manassas, VA), athymic nude mice (nu/nu, half male and half female, 4−6 weeks of age, 18−20 g; Charles River Laboratories, Shanghai, China), and materials for cell culture were purchased from commercial sources.

2.2. Synthesis of Quaternary ZAISe QDs. For a typical synthetic reaction, $Zn(Ac)_2$ (0.1 mmol), $AgNO_3$ (0.1 mmol), and $In(Ac)_3$ (0.1 mmol) were mixed with 4 mL of ODE, 0.5 mL of DDT, and 50 μL of OA in a 50 mL three-neck flask. While being mildly stirred, the reaction mixture was slowly heated to 175 °C over 10 min under a nitrogen atmosphere until a clear solution was obtained. At this time, the Se precursor solution prepared by dissolving 0.3 mmol of Se powder in the mixture of oleylamine (0.5 mL) and dodecanethiol (0.2 mL) was injected with a syringe.[30] The solution turned immediately to dark. The reaction temperature was kept at 175 °C for 30 min to allow the growth of $ZnAgInSe_3$ QDs. After that, the flask was rapidly cooled to room temperature to harvest QD products. The resulting QDs could be separated by ethanol precipitation, and they could be re-dispersed in *n*-decane, toluene, hexane, chloroform, ether, etc. In this study, we fully investigated the influence of the reacting temperature and time, the DDT amount, and the Ag/Zn feed ratio on the preparation of quaternary QDs.

2.3. Synthesis of RGD-Modified SOC Micelles. RGD-SOC (*N*-succinyl-*N*′-octyl-chitosan) micelles used for the water transfer of oil-soluble quaternary ZAISe QDs were prepared via a two-step method, as follows.

2.3.1. Synthesis of SOC Micelles. SOC micelles were prepared according to our previous reports.[13,25] After dialysis and lyophilization, the powder of SOC micelles was obtained.

2.3.2. RGD Peptide Modification of SOC Micelles. The RGD peptide with more favorable water solubility was used to replace folic acid reported previously[13,25] for the surface modification of SOC micelles (Figure 1b). Briefly, the COOH group of monomeric cyclic RGD-succinic acid [5 mg, monomeric cyclic RGD-succinic acid was prepared by the reaction between monomeric cyclic RGD peptide and succinic anhydride in dimethylformamide (Figure S5 of the Supporting Information)] was activated by an EDC/NHS catalyst system (RGD-succinic acid/EDC/NHS molar ratio of 1/1.5/1.5) in water (2.5 mL) and then added dropwise to react with free amino groups on the surfaces of SOC micelles. After further purification by dialysis (molecular weight cutoff of 10000) against deionized water, RGD-modified SOC micelles were prepared.

2.4. Water Solubilization. The resulting quaternary oil-soluble ZAISe QDs (50 μL, ∼0.6 mg) could be successfully transferred into water (1 mL) using RGD-SOC micelles (∼3 mg), using the recently reported method.[13] Finally, the clear water solution of QD-loaded RGD-SOC micelles after centrifugation was stored at room temperature (or at 4 °C) for subsequent research.

2.5. Characterization. An S2000 eight-channel optical fiber spectrophotometer (Ocean Optics, Inc.), an X-Cite Series 120Q broadband light source (Lumen Dynamics Group Inc.), an NL-FC-

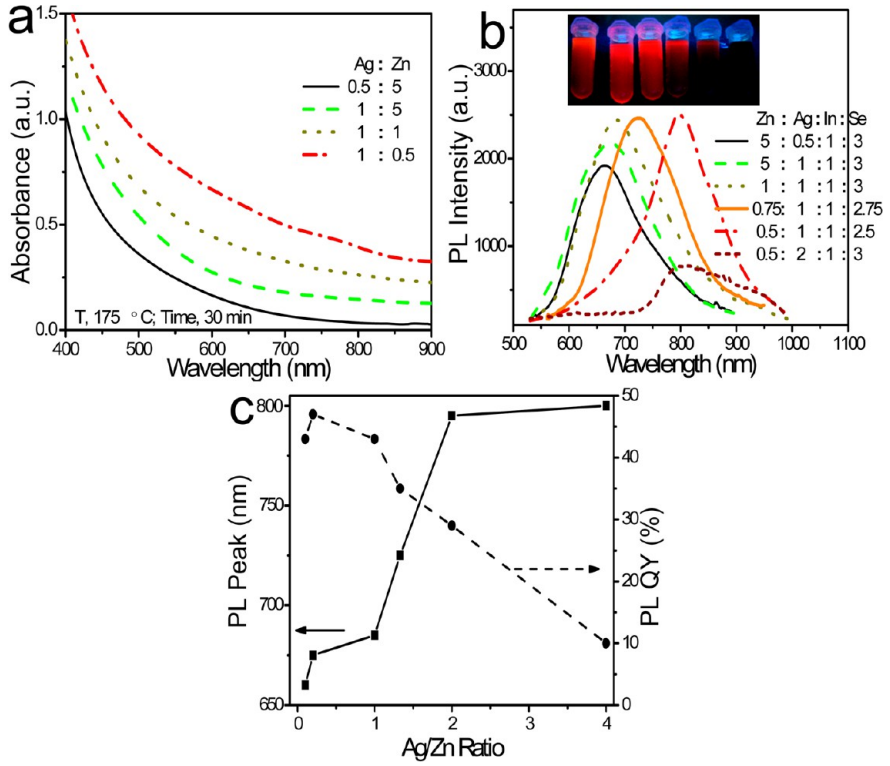

Figure 2. (a) Absorption and (b) photoluminescence (PL) spectra of the dispersions of quaternary ZAISe QDs prepared with various Ag/Zn feed ratios. The inset of panel b shows the true-color fluorescent images of the as-prepared QD solutions taken under the excitation of a UV lamp. (c) PL peak and PL QY of quaternary ZAISe QDs vs the Ag/Zn feed ratio.

2.0-766 semiconductor laser (λ = 766 nm; Enlight), and a PerkinElmer UV–vis spectrometer were employed for the measurements of optical spectra at room temperature. The PL QY of QDs was determined by further following the previously reported method.[13,28,29,31]

A transmission electron microscope operating at 200 kV (JEOL JEM-2100) and a laser particle size analyzer (LPSA) (Mastersizer 2000, Malvern) were combined to characterize the size and shape of samples. Energy-dispersive spectroscopy (EDS) and X-ray photoelectron spectroscopy (XPS) (PHI5000 VersaProbe, ULVAC-PHI Inc.) were used to determine the elemental compositions of QDs. The powder XRD experiment was performed on a Philips X'Pert PRO X-ray diffractometer to detect the crystal structure of QDs.

2.6. *In Vitro* Cell Imaging. MDA-MB-231 (or MCF-7) cells were first seeded on a confocal Petri dish and incubated in RPMI 1640 medium with 10% (v/v) calf serum at 37 °C (5% CO_2). After incubation for 24 h, the medium was removed, and then 200 μL of fresh RPMI 1640 medium containing QD-loaded RGD-SOC micelles (~10 μg/mL QDs) was added. After incubation for an additional 9 h, the medium was removed again, and the cells were washed with phosphate-buffered saline (PBS) (three times, 5 min each). The Olympus Fluoview 300 confocal laser scanning system (λ_{ex} = 488 nm) was used to acquire the fluorescence images of cells.

2.7. *In Vivo* Animal Imaging. In brief, first, MDA-MB-231 (or MCF-7) cells were injected subcutaneously into the right armpit of each nude mouse. When the tumors grew to 0.4–0.6 cm in diameter, the mice were ready for *in vivo* NIR imaging experiments. In a typical imaging experiment, 200 μL of QD-loaded RGD-SOC micelles (the dose of QDs, ~10 μg/g of body weight) was administered intravenously into each tumor-bearing nude mouse (n = 3 for each group). Next, the mice were imaged at various time points (0–12 h) post-injection with a homemade *in vivo* small animal NIR imaging system (see the previous reports for more details on imaging and animal management rules[13,25,26]).

3. RESULTS AND DISCUSSION

This work addresses the synthesis and bio-application of high-quality oil-soluble quaternary ZAISe QDs; thus, the results and discussion is divided into three parts. As depicted in the overall synthetic scheme in Figure 1a, the synthesis of oil-soluble quaternary ZAISe QDs is presented in section 3.1, in which main parameters influencing the optical properties of quaternary QDs were explored systematically. Next, synthesizing an RGD peptide-modified SOC micelle and using it as phase transfer agent, we transferred the prepared high-quality oil-soluble quaternary ZAISe QDs into water (section 3.2), based on the hydrophobic interaction between the octyl groups of the micelle and the dodecanethiol molecules on the QD surface. At last, using multiscale optical imaging techniques, these quaternary QDs were investigated further to determine whether they can be applied as a versatile fluorescent probe to visually assess the targeting capability of micelles to tumor cells and tissue (section 3.3).

3.1. Synthesis and Optical Properties of Oil-Soluble Quaternary ZAISe QDs. A challenge in synthesizing colloidal I–III–VI or Zn–I–III–VI nanocrystals (NCs) is their ternary or quaternary composition, compared with that of traditional binary II–VI, IV–VI, and III–V NCs.[9−11] In this study, we use the reactivity-controlling ligand dodecanethiol (DDT) reported by Peng et al.[11] to balance the reactivity of cationic precursors (namely, Ag and In), because they had higher reactivity than zinc in the reaction with selenium.[32] By further combining the recent report that the Se powder dissolved in the mixture of oleylamine (OLA) and DDT (i.e., the Se precursor solution) can be used as a favorable selenium source for the synthesis of selenide nanocrystals,[30] we developed a new facile one-pot strategy for preparing oil-soluble quaternary ZAISe QDs (see

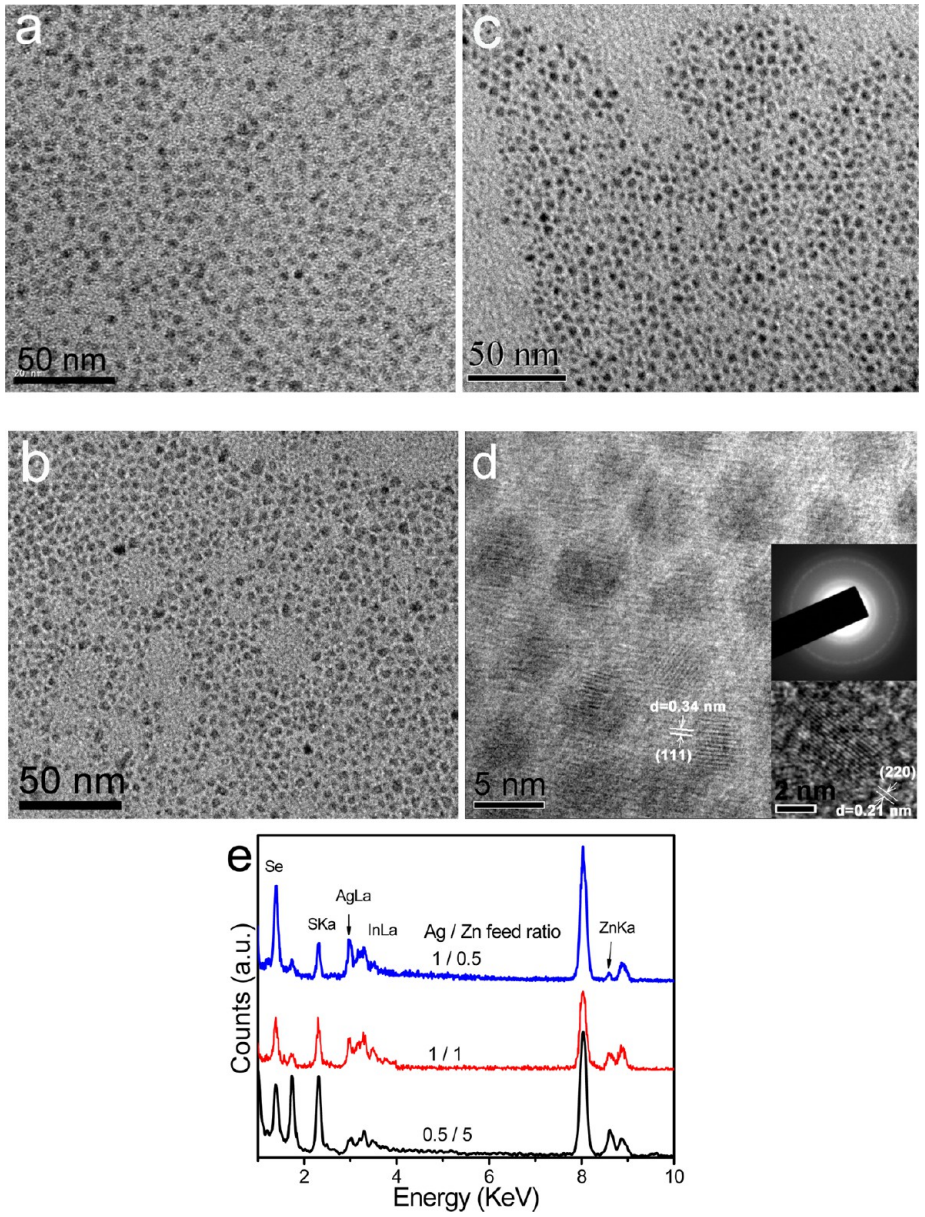

Figure 3. TEM images of quaternary ZAISe QDs prepared with different Ag/Zn feed ratios: (a) 0.5/5, (b) 1/1, and (c) 1/0.5. (d) High-resolution TEM images and SAED pattern of the as-prepared $ZnAgInSe_3$ QDs. Two sets of lattice planes with *d* spacings of 0.34 and 0.21 nm can be clearly identified and should correspond to the (111) and (220) lattice planes of the cubic structure. Meanwhile, the three diffraction rings in the SAED pattern can also be readily assigned to the (111), (220), and (311) planes of a cubic structure. (e) Corresponding energy-dispersive X-ray (EDX) spectra of the samples in panels a–c.

Figure S1 of the Supporting Information). The PL and absorption spectra of quaternary ZAISe QDs are observed to be broad and have no well-defined exciton absorption peak, respectively, although the as-produced QDs have a narrow size distribution as discussed below. These might be the typical indicative features of quaternary compounds, which should be attributed to the unique electronic properties and the inhomogeneity of the elemental distribution among various quaternary QDs in an ensemble.[19−23]

The series of experimental data are displayed in Figure 2 and Figure S2 of the Supporting Information, in which several crucial variables, e.g., reaction temperature, growth time, the amount of DDT, and the Ag/Zn feed ratio, were varied in an orderly fashion. As shown, the reaction temperature of 175 °C, the reaction time of 30 min, and the amount of DDT of 0.7 mL (i.e., 0.7 = 0.5 + 0.2) are optimal for achieving highly luminescent quaternary ZAISe QDs (the detailed explanations for these experimental parameters are provided in the Supporting Information). More importantly, some interesting results are observed, as follows. (i) The OLA−Se complexes formed by dissolving Se powder in the mixture of OLA and DDT are highly reactive. Even at 90 °C, the OLA−Se complexes can react with Zn^{2+}, Ag^{+}, and In^{3+} to form quaternary ZAISe QDs. (ii) With the extension of the reaction time or the increase in the reaction temperature, no obvious blue shifts in the PL peak of QDs are observed, which suggests that homogeneous quaternary ZAISe nuclei with certain compositions are formed directly by the reaction between cations and selenium with the additional assistance of the cation reactivity-controlling ligand DDT.[11] That is to say, in the

growth process in which $AgInSe_2$ nucleates first and subsequently zinc gradually diffuses into QDs in the crystal growth stage, thish should not be the principal formation mechanism of quaternary ZAISe QDs in this synthesis system (the band gaps of bulk $AgInSe_2$ and ZnSe are 1.24 and 2.7 eV, respectively[9,33]).[17−20] (iii) It is found that with a change in the Ag/Zn feed ratio from 0.5/5 to 2/0.5, the PL peak of the resulting quaternary ZAISe QDs can be conveniently tuned from 660 to 800 nm [the maximal PL QY is close to ∼50% (PL peak, 675 nm)], and the corresponding absorption spectra also red-shift gradually (Figure 2).

Next, major efforts were focused on investigating and revealing the important role of the Ag/Zn feed ratio for the synthesis of the quaternary ZAISe QDs by TEM, XRD, EDAX, and XPS. TEM images in Figure 3a−c show that the as-produced QDs have a narrow size distribution and all of the QDs samples had a similar particle size (∼5 nm in diameter), which could exclude the effect of size on the shift of the band edge. The data in Figures 3d and 4 indicate that the obtained

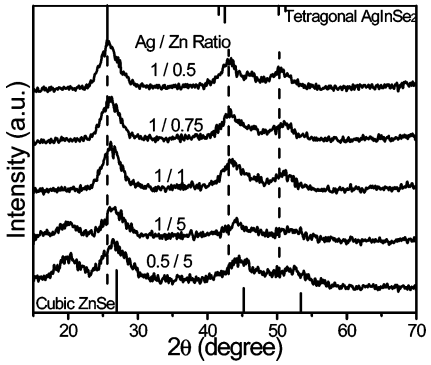

Figure 4. XRD patterns of quaternary Zn−Ag−In−Se QDs prepared with different Ag/Zn feed ratios.

quaternary QDs had a cubic crystal structure (zinc blende). Furthermore, the three major diffraction peaks were generally between the main XRD peaks of chalcopyrite $AgInSe_2$ and cubic ZnSe and systematically shifted toward higher angles with the Ag/Zn feed ratio decreasing from 1/0.5 to 0.5/5. These results reveal that quaternary ZAISe QDs have been prepared successfully, and their compositions can be tuned by controlling the Ag/Zn feed ratio used, which has been further proven by the quantitative elemental analyses of the QDs by EDX (Figure 3e) and XPS (Figure S3 of the Supporting Information).

On the basis of the analyses described above, we can conclude that highly luminescent oil-soluble quaternary ZAISe QDs have been prepared, and their PL maximum can be conveniently adjusted from 660 to 800 nm by increasing the Ag/Zn feed ratio. The spectral shifts induced by the change in the Ag/Zn feed ratio should be mainly ascribed to the resultant alteration in the QD composition. This result further enriches our understanding of the QD synthesis that different from binary QDs, for quaternary Zn−I−III−VI semiconductor QDs, their compositions might play a more crucial role in controlling the PL peak position, as observed recently by us and other groups.[19−23]

3.2. Water Solubilization of Oil-Soluble Quaternary ZAISe QDs via RGD-SOC Micelles. The as-synthesized quaternary Zn−Ag−In−Se QDs coated by one monolayer of dodecanethiol molecules because of the coordination between thiol group and cations on the QD surfaces are hydrophobic. To expand further their applications in bioimaging, RGD peptide-modified SOC (RGD-SOC) micelles were prepared and used as a water transfer agent (Figure 1b). Here, the RGD-modified chitosan-based micelles were selected as a drug carrier model because they are a promising targeted drug delivery system based on the facts that (i) chitosan, a plentiful natural biopolymer, is suitable for the fabrication of a biocompatible micelle because of good biocompatibility, low cytotoxicity, and biodegradability, as well as the high amine group content of its backbone,[24,25] and (ii) the RGD peptide has been demonstrated to have a high affinity for the $\alpha_v\beta_3$ integrin receptor, a family of cell surface glycoproteins consisting of two non-covalently bound transmembrane subunits (α and β),[34] and may serve as the ligand to promote the accumulation of the anticancer drug or drug carrier in $\alpha_v\beta_3$ integrin receptor overexpressed malignant cells.[23] In addition, another important reason for using RGD-SOC micelles in this study to replace folate-modified SOC micelles reported previously by us is that the RGD peptide is more water-soluble than folate. Thus, after modification, the RGD groups should mainly be located on the

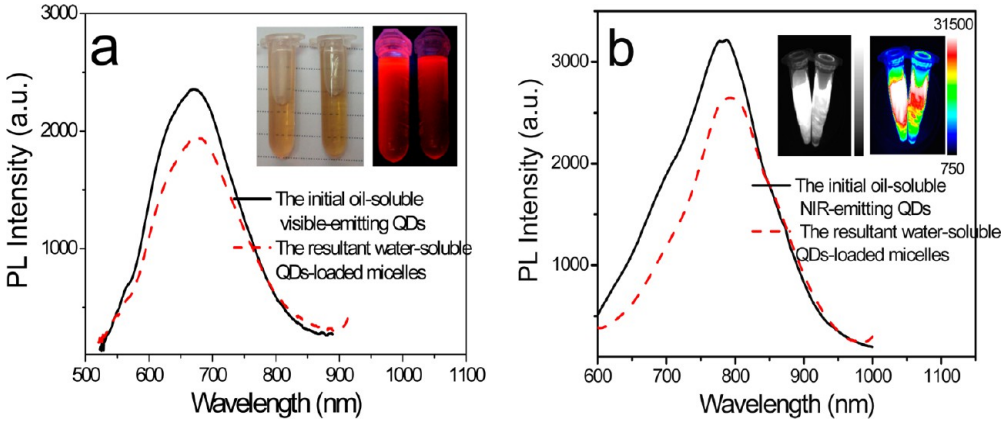

Figure 5. PL spectra of visible light-emitting (a) (λ_{ex} = 470 nm) and NIR-emitting (b) (λ_{ex} = 520 nm) quaternary ZAISe QDs in *n*-decane and after water transfer via RGD-SOC micelles. Insets of panel a are the true-color images of initial visible light-emitting QDs and resultant QD-loaded micelles taken under room light and UV light excitation. Insets of panel b are the black-and-white and pseudocolored images, respectively, of initial NIR-emitting QDs and resultant QD-loaded micelles taken under NIR laser light (λ_{max} = 766 nm).

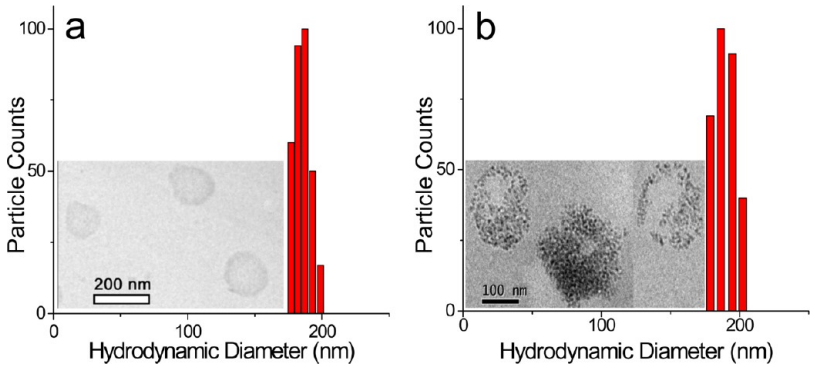

Figure 6. Size distributions of (a) initial RGD-SOC micelles and (b) resultant QD-loaded micelles by DLS. Insets of panels a and b are the corresponding TEM images.

surfaces of micelles, and the free RGD peptide will not be uploaded into the hydrophobic cores of micelles.

Figure 1 shows the overall synthetic scheme for the fabrication of the RGD-SOC micelles and the corresponding water transfer of oil-soluble quaternary ZAISe QDs. After chemical modification with succinic acid and octaldehyde, the obtained chitosan-based polymer molecules are amphiphilic and will self-assemble into a spherical micelle possessing a hydrophobic core and a hydrophilic shell, in which the RGD peptide was used further to functionalize the surface of the SOC micelle. The hydrophobic interaction makes the oil-soluble QDs upload spontaneously into the cores of micelles, achieving the water transfer of oil-soluble quaternary ZAISe QDs. The PL spectra of ZAISe QDs before and after water transfer via micelles were measured and are shown in Figure 5. These data not only confirm that by using RGD-SOC micelles, the hydrophobic ZAISe QDs could be transferred successfully into water but also indicate that after water solubilization, the main PL properties (e.g., PL intensity and PL peak position; typically, the PL QY of the resulting QD-loaded micelles is approximately 20−30%) of initial quaternary QDs could be retained. For the sake of clarity, the corresponding optical images of the studied samples taken under different excitation light sources are presented in the insets of Figure 5.

Next, TEM and dynamic light scattering (DLS) were used further to characterize the sizes (or size distributions) and shapes of initial RGD-SOC micelles and resulting QD-loaded micelles. As presented in panels a and b of Figure 6, the uploading of hydrophobic QDs into micelles does not have a strong influence on the average hydrodynamic diameter of micelles (~180 nm). TEM images in Figure 6 show that the initial spherical RGD-SOC micelles (with hollow interiors) were loaded with oil-soluble QDs when they were mixed with hydrophobic QDs, confirming the formation of the QD−micelle nanocomposites, in which the size, morphology, and crystal structure of the initial oil-soluble QDs were retained (Figures 3 and 6 and Figure S4 of the Supporting Information). It is noteworthy that different from the uploading of oil-soluble QDs via folate-SOC micelles (in which the free folate with hydrophobicity and oil-soluble QDs might be packed together into the cores of micelles),[13] here, the hydrophobic interaction between the octyl groups of the micelle and the DDT molecules on the QD surface as depicted schematically in Figure 1 make the QDs assemble to the inner surface of RGD-SOC micelles, because the RGD peptide used with favorable water solubility will not interfere with the uploading of oil-soluble QDs. That is, the cores of the nanocomposites are empty (Figure S4 of the Supporting Information). Thus, the empty cores of the QD−micelle nanocomposites could be used further to load other hydrophobic molecules, e.g., hydrophobic anticancer drugs. Therefore, the as-prepared fluorescent QD−micelle nanocomposites have great potential to be used further in the optical imaging (or tracing) of hydrophobic drugs. The loading capacity of RGD-SOC micelles for oil-soluble QDs can be close to ~30%.[13] In addition, the PL intensity of the QD-loaded micelles in water decreased only ~20% after one week of storage, which helps in their further application as unique fluorescent materials for bioimaging.

3.3. Multiscale Biomedical Imaging Using Oil-Soluble Quaternary ZAISe QDs. The RGD-modified chitosan-based micelles are a promising targeted delivery carrier for hydrophobic anticancer agents. However, this class of molecules does not produce a detectable fluorescence signal. According to the previous studies,[23−27] to assess their targeting ability to $\alpha_v\beta_3$ integrin receptor-positive tumors, two dyes with various fluorescent emissions must be used, that is, visible dye for cell imaging and NIR dye for animal imaging. In this study, we noted that the quaternary ZAISe QDs exhibited strongly luminescent emission, had a widely tunable spectral region (from 660 to 800 nm), and could be conveniently transferred into water by RGD-SOC micelles, and the as-prepared QD-loaded micelles showed low cytotoxicity assessed by the MTT assay (see Figure S7 of the Supporting Information). Hence, next, the application of the highly luminescent quaternary QDs for *in vitro* and *in vivo* evaluation of the tumor targeting capability of RGD-SOC micelles was explored further.

To confirm their potential for *in vitro* optical imaging of the distribution of micelles within cells, $\alpha_v\beta_3$ integrin receptor-positive MDA-MB-231 cells and $\alpha_v\beta_3$ integrin receptor-negative MCF-7 cells were used for co-incubation with QD-loaded RGD-SOC micelles (λ_{em} = 675 nm). The representative LCSM images of MDA-MB-231 and MCF-7 cells cultured with the OD-loaded micelles are shown in panels a and b of Figure 7, respectively. As shown, after incubation for 9 h, a significant number of QD-loaded RGD-SOC micelles were internalized and mainly accumulated in the cytoplasm by phagocytosis of MDA-MB-231 cells (Figure 7a). In contrast, the sites of $\alpha_v\beta_3$-negative MCF-7 cells (Fig. 7b) do not exhibit the significant specific fluorescent signal because of the low level of expression of the integrin receptor, which might indicate the receptor-mediated endocytosis of the RGD-SOC micelles. Meanwhile, these images also demonstrate the potential of the produced highly luminescent quaternary QDs for *in vitro* cell imaging.

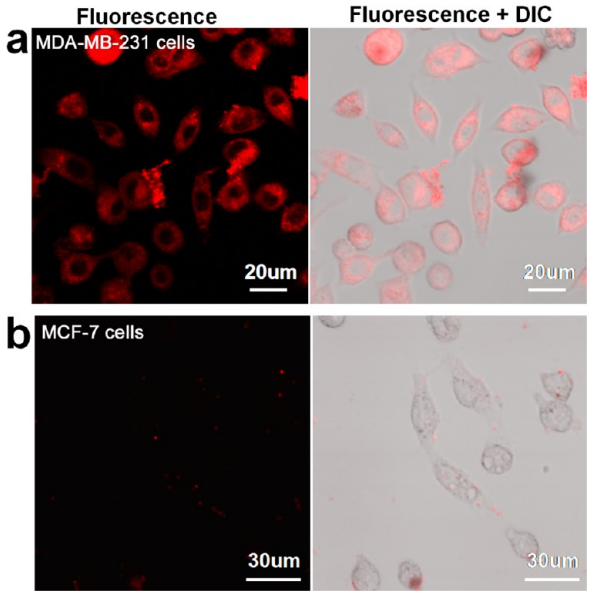

Figure 7. Laser confocal scanning microscopy (LCSM) images of (a) $\alpha_v\beta_3$-positive MDA-MB-231 cells and (b) $\alpha_v\beta_3$-negative MCF-7 cells after they had been incubated with 675 nm emitting QD−micelle nanocomposites (λ_{ex} = 488 nm).

In this section, we explore further the performance of these highly luminescent quaternary ZAISe QDs for *in vivo* imaging of the micelles in mouse, in which NIR-emitting QDs (λ_{em} = 790 nm) were used to replace red-emitting QDs. The RGD-SOC micelles loaded with NIR QDs were injected into nude mice bearing the $\alpha_v\beta_3$ integrin receptor-positive MDA-MB-231 tumor or the $\alpha_v\beta_3$ integrin receptor-negtive MCF-7 tumor via intravenous administration. Subsequently, a self-built small animal NIR imaging system was used to capture the *in vivo* NIR fluorescence images of mice at various time points post-injection (P.I.) (Figure 8a,b). As presented in Figure 8a, the detected background fluorescence under the excitation 766 nm laser light was quite weak before injection; 4 h P.I., a visible accumulation of the fluorescence signal at the tumor site and the liver was detected for the nude mice bearing the $\alpha_v\beta_3$-positive MDA-MB-231 tumor, while more than 10 h P.I., the magnitudes of the fluorescence signals in the tumor and liver gradually decreased. Nevertheless, injecting the same dose of NIR QD−micelle nanocomposites into nude mice bearing the $\alpha_v\beta_3$-negtive MCF-7 tumor did not induce a similar accumulation of fluorescence signal at the tumor site (Figure 8b). The corresponding temporal evolution curves of T/N ratios of QD-loaded RGD-SOC micelles in MDA-MB-231 and MCF-7 tumor-bearing nude mice are shown in Figure 8c. These data from *in vivo* NIR imaging experiments demonstrate the high *in vivo* targeting capability of RGD-modified micelles to the $\alpha_v\beta_3$ integrin receptor-positive tumor. On the other hand, these results confirm further the potential of the produced highly luminescent quaternary QDs for *in vivo* animal imaging.

Caution: *The use of the quaternary ZAISe QDs for bioimaging should be limited to cells and small animals at low doses because of the likely potential toxicity.*

4. CONCLUSIONS

In summary, by systematically optimizing reaction parameters, we prepared high-quality quaternary ZAISe QDs via a new facile one-pot strategy. These oil-soluble quaternary QDs have bright PL emission (PL QY of close to 50%) as well as a widely tunable PL maximum in the region from 660 to 800 nm. With RGD-SOC micelles, these hydrophobic quaternary QDs can be successfully uploaded and transferred into water, in which the shape, crystal structure, and optical properties of initial QDs were kept. By optical imaging techniques, the quaternary ZAISe QDs prepared were demonstrated to have the potential as a versatile fluorescent probe for multi-spatial scale biomedical imaging of micelles. This study is particularly significant for developing new biocompatible quaternary QDs to replace binary Cd- and Pb-based QDs for biomedical applications.

■ ASSOCIATED CONTENT

Supporting Information

Additional information about the synthesis and bioapplication of the quaternary QDs, such as absorption and PL spectra, XPS spectra, TEM images, etc. (Figures S1−S7). This material is available free of charge via the Internet at http://pubs.acs.org.

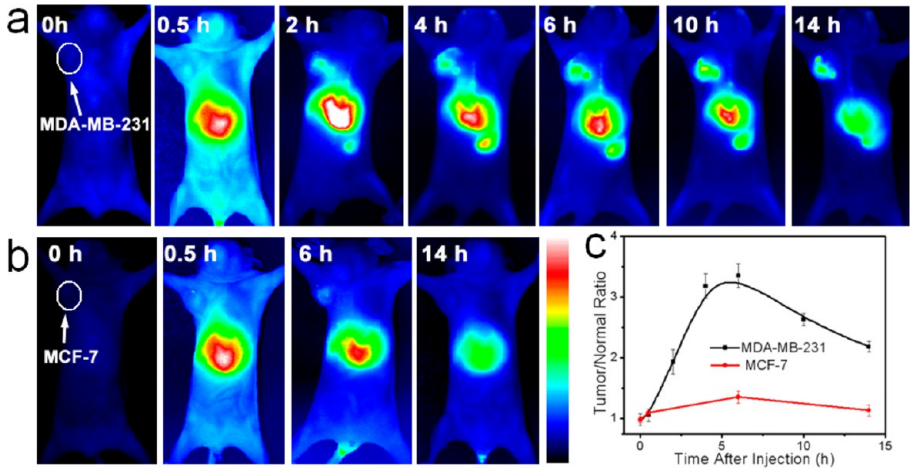

Figure 8. Dynamic distributions of NIR QD-loaded RGD-SOC micelles in nude mice bearing (a) the $\alpha_v\beta_3$-positive MDA-MB-231 tumor or (b) the $\alpha_v\beta_3$-negtive MCF-7 tumor monitored by the NIR fluorescence imaging system. (c) Corresponding temporal evolution curves of tumor-to-normal tissue (T/N) ratios of NIR QD-loaded RGD-SOC micelles in MDA-MB-231 and MCF-7 tumor-bearing nude mice.

AUTHOR INFORMATION

Corresponding Authors

*E-mail: dengdawei@cpu.edu.cn.
*E-mail: zjian@umich.edu.
*E-mail: guyueqingsubmission@hotmail.com.

Notes

The authors declare no competing financial interest.

ACKNOWLEDGMENTS

This study was financially supported by the Program for New Century Excellent Talents (NCET-12-0974) of the Ministry of Education of China, the National Natural Science Foundation of China (81371627 and 81220108012), and the Natural Science Foundation of Jiangsu Province (BK20116394). Our thanks to Prof. Samuel Achilefu (Washington University, St. Louis, MO) for the NIR dye cypate.

REFERENCES

(1) Achilefu, S. *Chem. Rev.* **2010**, *110*, 2575−2578.
(2) Willmann, J. K.; van Bruggen, N.; Dinkelborg, L. M.; Gambhir, S. S. *Nat. Rev. Drug Discovery* **2008**, *7*, 591−607.
(3) Kim, S.; Lim, Y. T.; Soltesz, E. G.; De Grand, A. M.; Lee, J.; Nakayama, A.; Parker, J. A.; Mihaljevic, T.; Laurence, R. G.; Dor, D. M.; Cohn, L. H.; Bawendi, M. G.; Frangioni, J. V. *Nat. Biotechnol.* **2004**, *22*, 93−97.
(4) Frangioni, J. V. *Curr. Opin. Chem. Biol.* **2003**, *7*, 626−634.
(5) Singh, A.; Lim, C. K.; Lee, Y. D.; Maeng, J.; Lee, S.; Koh, J.; Kim, S. *ACS Appl. Mater. Interfaces* **2013**, *5*, 8881−8888.
(6) Michalet, X.; Pinaud, F. F.; Bentolila, L. A.; Tsay, J. M.; Doose, S.; Li, J. J.; Sundaresan, G.; Wu, A. M.; Gambhir, S. S.; Weiss, S. *Science* **2005**, *307*, 538−544.
(7) Smith, A. M.; Duan, H.; Mohs, A. M.; Nie, S. *Adv. Drug Delivery Rev.* **2008**, *60*, 1226−1240.
(8) Pons, T.; Pic, E.; Lequeux, N.; Cassette, E.; Bezdetnaya, L.; Guillemin, F.; Marchal, F.; Dubertret, B. *ACS Nano* **2010**, *4*, 2531−2538.
(9) Zhong, H. Z.; Bai, Z. L.; Zou, B. S. *J. Phys. Chem. Lett.* **2012**, *3*, 3167−3175.
(10) Pradhan, N.; Sarma, D. D. *J. Phys. Chem. Lett.* **2011**, *2*, 2818−2826.
(11) Xie, R. G.; Rutherford, M.; Peng, X. G. *J. Am. Chem. Soc.* **2009**, *131*, 5691−5697.
(12) Li, L.; Pandey, A.; Werder, D. J.; Khanal, B. P.; Pietryga, J. M.; Klimov, V. I. *J. Am. Chem. Soc.* **2011**, *133*, 1176−1179.
(13) Deng, D. W.; Chen, Y. Q.; Cao, J.; Tian, J. M.; Qian, Z. Y.; Achilefu, S.; Gu, Y. Q. *Chem. Mater.* **2012**, *24*, 3029−3037.
(14) Cassette, E.; Pons, T.; Bouet, C.; Helle, M.; Bezdetnaya, L.; Marchal, F.; Dubertret, B. *Chem. Mater.* **2010**, *22*, 6117−6124.
(15) Yu, K.; Ng, P.; Ouyang, J.; Zaman, M. B.; Abulrob, A.; Baral, T. N.; Fatehi, D.; Jakubek, Z. J.; Kingston, D.; Wu, X.; Liu, X.; Hebert, C.; Leek, D. M.; Whitfield, D. M. *ACS Appl. Mater. Interfaces* **2013**, *5*, 2870−2880.
(16) Torimoto, T.; Adachi, T.; Okazaki, K.; Sakuraoka, M.; Shibayama, T.; Ohtani, B.; Kudo, A.; Kuwabata, S. *J. Am. Chem. Soc.* **2007**, *129*, 12388−12389.
(17) Tang, X. S.; Yu, K.; Xu, Q. H.; Choo, E. S. G.; Goh, G. K. L.; Xue, J. M. *J. Mater. Chem.* **2011**, *21*, 11239−11243.
(18) Tang, X. S.; Ho, W. B. A.; Xue, J. M. *J. Phys. Chem. C* **2012**, *116*, 9769−9773.
(19) Zhang, J.; Xie, R. G.; Yang, W. S. *Chem. Mater.* **2011**, *23*, 3357−3361.
(20) Sarkar, S.; Karan, N. S.; Pradhan, N. *Angew. Chem., Int. Ed.* **2011**, *50*, 6065−6069.
(21) Feng, J.; Sun, M.; Yang, F.; Yang, X. R. *Chem. Commun.* **2011**, *47*, 6422−6424.
(22) Manna, G.; Jana, S.; Bose, R.; Pradhan, N. *J. Phys. Chem. Lett.* **2012**, *3*, 2528−2534.
(23) Deng, D. W.; Cao, J.; Qu, L. Z.; Achilefu, S.; Gu, Y. Q. *Phys. Chem. Chem. Phys.* **2013**, *15*, 5078−5083.
(24) Bhattarai, N.; Gunn, J.; Zhang, M. *Adv. Drug Delivery Rev.* **2010**, *62*, 83−99.
(25) Zhu, H. Y.; Liu, F.; Guo, J.; Xue, J. P.; Qian, Z. Y.; Gu, Y. Q. *Carbohydr. Polym.* **2011**, *86*, 1118−1129.
(26) Cao, J.; Cui, S. S.; Li, S. W.; Du, C. L.; Chen, W. R.; Tian, J. M.; Wan, S. N.; Qian, Z. Y.; Gu, Y. Q. *Cancer Res.* **2013**, *73*, 1362−1373.
(27) Deng, D. W.; Zhang, D. Y.; Li, Y.; Achilefu, S.; Gu, Y. Q. *Biosens. Bioelectron.* **2013**, *49*, 216−221.
(28) Ye, Y. P.; Bloch, S.; Kao, J.; Achilefu, S. *Bioconjugate Chem.* **2005**, *16*, 51−61.
(29) Ye, Y. P.; Bloch, S.; Xu, B.; Achilefu, S. *Bioconjugate Chem.* **2008**, *19*, 225−234.
(30) Liu, Y.; Yao, D.; Shen, L.; Zhang, H.; Zhang, X.; Yang, B. *J. Am. Chem. Soc.* **2012**, *134*, 7207−7210.
(31) Deng, D. W.; Qu, L. Z.; Li, Y.; Gu, Y. Q. *Langmuir* **2013**, *29*, 10907−10914.
(32) Moon, G. D.; Ko, S.; Min, Y.; Zeng, J.; Xia, Y. N.; Jeong, U. *Nano Today* **2011**, *6*, 186−203.
(33) Cao, J.; Xue, B.; Li, H.; Deng, D. W.; Gu, Y. Q. *J. Colloid Interface Sci.* **2010**, *348*, 369−376.
(34) Achilefu, S.; Bloch, S.; Markiewicz, M. A.; Zhong, T.; Ye, Y.; Dorshow, R. B.; Chance, B.; Liang, K. *Proc. Natl. Acad. Sci. U.S.A.* **2005**, *102*, 7976−7981.